Available online at www.sciencedirect.com

ScienceDirect

Acta Materialia 66 (2014) 199–208

Acta MATERIALIA

www.elsevier.com/locate/actamat

Microstructural evolution during ageing of Al–Cu–Li–x alloys

Vicente Araullo-Peters [a,b,*], Baptiste Gault [c], Frederic de Geuser [d], Alexis Deschamps [d], Julie M. Cairney [a,b]

[a] School of Aerospace Mechanical and Mechatronic Engineering, University of Sydney, Sydney, Australia
[b] Australian Centre for Microscopy and Microanalysis, University of Sydney, Sydney, Australia
[c] Department of Materials, University of Oxford, Parks Road, Oxford OX1 3PH, UK
[d] SIMaP, Grenoble INP-UJF-CNRS, Saint-Martin-d'Heres, France

Received 23 September 2013; received in revised form 4 December 2013; accepted 4 December 2013
Available online 9 January 2014

Abstract

In this study, atom probe tomography was used to investigate the microstructure of the alloy AA2198 (Al–1.35 Cu–3.55 Li–0.29 Mg–0.08 Ag) over a range of ageing conditions to examine the evolution of phases in the alloy, in particular aiming to reveal the nucleation mechanism of the strengthening T_1 phase. T_1 precursor phases were observed from early ageing, most of which were connected to dislocations enriched with Mg and Ag. This Mg solute segregation on the dislocations was subsequently observed to develop into S-like phases. Ag and Mg segregation to T_1 interfaces was systematically observed when the plates were oriented perpendicular to the probing direction. The matrix solute content was followed during the course of T_1 precipitation. It was found that the evolution of Cu, Li, Mg and Ag was similar, giving additional evidence for their co-precipitation.

Keywords: Atom probe tomography; Precipitation hardening; AA2198; T1 phase; Crystallography

1. Introduction

Aluminium lithium alloys are of great interest for commercial, military and aerospace applications due to their excellent combination of low density, high stiffness and high strength [1–3]. For aluminium alloys, Li provides the largest reduction in density and greatest increase in stiffness per percentage weight of any known alloying element [4]. Every 1 at.% of Li added to the alloy reduces the total density of the alloy by 3% and the Li solubility in aluminium is ~4.2 at.% [5]. When other solutes are added, particularly Cu, the strengthening potential of Al–Li alloys becomes remarkable as a result of the sophisticated combination of phases that form during processing (Table 1 lists some of the phases commonly found in these alloys). In order to improve the properties of Al–Li–Cu alloys through the design of appropriate compositions and thermomechanical processing regimes, it is therefore necessary to understand the complex microstructure within these alloys and the sequence of events that lead from the as-quenched supersaturated solid solution to the end microstructure.

The AA2198 alloy, whose composition is given in Table 2, has been shown to have a desirable combination of tensile properties, formability and damage tolerance [6]. These Al–Li–Cu alloys can be produced with high yield strength, which is attributed to the precipitation of the T_1 phase (Al_2LiCu). This phase forms as thin plates lying on the {1 1 1} matrix planes. Its structure as a bulk phase has been determined by Van Smaalen et al. [7] and its structure as a precipitate embedded in aluminium has been more recently established [8,9]. There are four reported nucleation sites for the phase: grain boundaries, zirconium dispersoids, octahedral voids/Guinier–Preston zones and dislocations [10]. Cold work prior to ageing has been

* Corresponding author at: School of Aerospace Mechanical and Mechatronic Engineering, University of Sydney, Sydney, Australia.
E-mail address: vicente.araullopeters@sydney.edu.au (V. Araullo-Peters).

1359-6454/$36.00
http://dx.doi.org/10.1016/j.actamat.2013.12.001

Table 1
Common phases in the Al–Li–Cu–Mg–Ag–Zr alloys.

Phase	Composition	Crystal structure	Common morphology
T_1	Al_2CuLi	Hexagonal	Plates
Θ'	Al_2Cu	Tetragonal	Plates
δ'	Al_3Li	Ll_2	Coating
β'	Al_3Zr	Ll_2	Dispersoid
S	Al_2CuMg	Orthorhombic	Laths, rods

Table 2
Composition of the AA2198 alloy.

Element	Li	Cu	Mg	Ag	Zr
Wt.%	0.8–1.1	2.9–3.5	0.25–0.8	0.1–0.5	0.04–0.18

shown to increase the amount of intra-granular precipitation of T_1 [11–13], which has been attributed to the increase in dislocation density and therefore potential nucleation sites in the form of high strain fields around kinks and jogs [14–16]. This is consistent with a model of T_1 nucleation where the plates are nucleated on the dissociation of a dislocation on opposite sides of a jog or cross-slipped screw segment [14].

Mg and Ag are known to aid T_1 precipitation and hence to improve the hardness of the alloy [13,16,17]. While a combination of Mg and Ag provides the greatest increase in hardness, alloying with Ag alone provides little gain. The distribution of these elements in the structure of the T_1 plates, as well as their partitioning between precipitates and matrix, as measured by atom probe, is the subject of conflicting reports. Some studies have shown the presence of Ag at the interface between the T_1 and the matrix [18], while others have not observed such interfacial segregation [19]. In a recent study, Decreus et al. [20] investigated in detail the precipitation sequence during ageing at 155 °C in AA2198 alloy using transmission electron microscopy (TEM) and small-angle X-ray scattering (SAXS). They provided evidence that the peak hardness microstructure consisted of thin T_1 platelets associated with a smaller fraction of Cu-rich phases (GPI, GPII and θ'). The sequence of events leading to this microstructure, as evidenced by in situ SAXS observations, involved first the dissolution of low-temperature clusters during the heating ramp to the ageing temperature, followed by an incubation time where no significant precipitation could be detected by this technique and, after ~2 h at 155 °C, sudden apparition and growth of the T_1 precipitates. From the available data, there was no indication of the mechanisms that could precede and accompany the nucleation of T_1 during this incubation time and during the subsequent precipitate growth.

The aim of the present study is to use state-of-the-art atom probe tomography (APT) and innovative data treatment methods to provide new insights into the microstructural evolution of the AA2198 structure at different ageing times, with particular emphasis on the early stages of precipitate nucleation when global characterization techniques such as SAXS [20] do not provide evidence of any detectable precipitation. APT is capable of determining the location and mass-to-charge ratio of atoms within volumes of ~100 nm × 100 nm × 500 nm with sub-nanometer resolution and can also be used to determine the orientation of the grains and the crystallographic features within them [21–26]. It is therefore a useful tool for examining the orientation and composition of the microstructural features in the early stages of ageing in the AA2198 alloy. The key concerns of this study are the location of Mg and Ag within the T_1 structure, the various T_1 nucleation sites and the interaction between T_1 precipitates, dislocations and other phases throughout all ageing conditions.

2. Experimental preparation and methods

Samples of AA2198, an alloy in the AIRWARE® family with a composition given in Table 2, were provided by the Constellium-Voreppe Research Centre, France. The AA2198 alloy was received in the T351 temper before being further aged. This involves solution treatment, water quenching, tensile predeformation to ~2% strain and then natural ageing for several months. The ageing treatment included a 20 K h^{-1} ramp up to 155 °C followed by isothermal annealing for 0, 1, 2, 15 or 84 h.

Atom probe specimens were prepared by standard electropolishing techniques with 25% perchloric acid and 70% glacial acetic acid at 14 V. Atom probe experiments were conducted with a Cameca LEAP® 3000X Si instrument operating in high-voltage pulsing mode at a base temperature of 20 ± 5 K and with a HV pulse amplitude 20% of the DC voltage applied to the specimen. Data reconstruction, using standard reconstruction algorithms [27], and three-dimensional (3-D) visualization was carried out using the commercial software IVAS™ (Cameca). Calibration of the tomograms was carried out using the methods introduced in Refs. [28,29].

The methods used for crystallographic characterization of specimens are described in detail in Refs. [21,25,30].

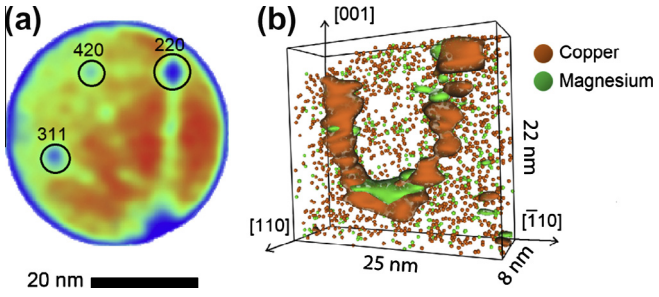

Fig. 1. (a) A 2-D density map of Al from a slice of the atom probe dataset, depicting the poles and therefore the orientation of the crystal grain. (b) A 3-D map showing part of a dislocation loop in an as-received AA2198 sample. A fraction of the Cu (orange) and Mg (green) atoms are shown, together with isoconcentration surfaces (Cu 3.6% in orange and Mg 1.6% in green) that highlight the loop due to the segregation of these elements. (For interpretation of the references to colour in this figure legend, the reader is referred to the web version of this article.).